Viral Infection of Tumors Overcomes Resistance to PD-1-immunotherapy by Broadening Neoantigenome-directed T-cell Responses

Norman Woller[1], Engin Gürlevik[1], Bettina Fleischmann-Mundt[1], Anja Schumacher[1], Sarah Knocke[1], Arnold M Kloos[1], Michael Saborowski[1], Robert Geffers[2], Michael P Manns[1], Thomas C Wirth[1], Stefan Kubicka[1,3] and Florian Kühnel[1]

[1]Clinic for Gastroenterology, Hepatology and Endocrinology, Hannover Medical School, Hannover, Germany; [2]Helmholtz Centre for Infection Research (HZI), Braunschweig, Germany; [3]Kreiskliniken Reutlingen, Reutlingen, Germany

There is evidence that viral oncolysis is synergistic with immune checkpoint inhibition in cancer therapy but the underlying mechanisms are unclear. Here, we investigated whether local viral infection of malignant tumors is capable of overcoming systemic resistance to PD-1-immunotherapy by modulating the spectrum of tumor-directed CD8 T-cells. To focus on neoantigen-specific CD8 T-cell responses, we performed transcriptomic sequencing of PD-1-resistant CMT64 lung adenocarcinoma cells followed by algorithm-based neoepitope prediction. Investigations on neoepitope-specific T-cell responses in tumor-bearing mice demonstrated that PD-1 immunotherapy was insufficient whereas viral oncolysis elicited cytotoxic T-cell responses to a conserved panel of neoepitopes. After combined treatment, we observed that PD-1-blockade did not affect the magnitude of oncolysis-mediated antitumoral immune responses but a broader spectrum of T-cell responses including additional neoepitopes was observed. Oncolysis of the primary tumor significantly abrogated systemic resistance to PD-1-immunotherapy leading to improved elimination of disseminated lung tumors. Our observations were confirmed in a transgenic murine model of liver cancer where viral oncolysis strongly induced PD-L1 expression in primary liver tumors and lung metastasis. Furthermore, we demonstrated that combined treatment completely inhibited dissemination in a CD8 T-cell-dependent manner. Therefore, our results strongly recommend further evaluation of virotherapy and concomitant PD-1 immunotherapy in clinical studies.

Received 24 February 2015; accepted 16 June 2015; advance online publication 21 July 2015. doi:10.1038/mt.2015.115

INTRODUCTION

Immunotherapy by blocking CTLA4 or PD-1/PD-L1 immune checkpoints has led to impressive tumor responses associated with significantly improved long-term survival in a subset of patients with advanced melanoma.[1–3] Although encouraging results have also been reported in other tumor entities,[1,4,5] the majority of cancer patients are refractory to immune checkpoint inhibitors. Factors that determine tumor susceptibility to checkpoint inhibition are not fully understood. In case of ipilimumab and its target CTLA-4 it has been suggested that pre-existing immune responses are an important precondition for successful checkpoint inhibition.[6,7] For PD-1/PD-L1 blockade, it is known that lymphocytic tumor infiltration as well as PD-L1 expression is associated with improved outcome in patients.[1] More recently, several groups demonstrated that tumor response was correlated with expression of PD-L1, particularly when expressed on tumor-infiltrating immune cells.[8,9] Furthermore, Tumeh *et al.*[10] showed that tumor responses to PD-1 blockade required pre-existing CD8 cells that were negatively regulated by PD-1/PD-L1-mediated adaptive immune resistance. It is assumed that neoantigens originating from gene mutations can serve as attractive targets of immunotherapy since they are not subject to central tolerance.[11,12] Consistently, it has been shown recently that those neoantigens are targeted by checkpoint blockade therapy.[13] Moreover, it has been reported that tumor regression in one patient with advanced melanoma involved a T-cell response against a particular neoantigen upon checkpoint blockade.[14] The sum of neoantigens of individual tumors can contain high numbers of potentially immunogenic epitopes. Due to the high frequency of mutations, melanoma has been a preferred target for immunotherapeutic approaches.[15] Analysis of peptides containing missense mutations from breast and colorectal cancer revealed that individual cancers accumulate an estimated number of up to 40–60 novel major histocompatibility complex class I (MHC I) restricted epitopes and on average 7–10 unique HLA-A*0201 epitopes, respectively, including those corresponding to mutated proteins involved in oncogenic processes.[16,17] On the other hand, tumors escape from immunosurveillance by establishing an immunosuppressive microenvironment[18] and also by immunoediting which shapes nascent tumors toward low immunogenicity.[12,19] Consequently, most cancers are usually devoid of highly immunogenic neoepitopes,

Correspondence: Norman Woller, Clinic for Gastroenterology, Hepatology and Endocrinology, Hannover, Medical School, Carl Neuberg Str. 1, D-30625 Hannover, Germany. E-mail: woller.norman@mh-hannover.de or Florian Kühnel, Clinic for Gastroenterology, Hepatology and Endocrinology, Hannover Medical School, Carl Neuberg Str. 1, D-30625 Hannover, Germany. E-mail: kuehnel.florian@mh-hannover.de

which makes them a challenging target for immunotherapies such as immune checkpoint modifiers.

Oncolytic viruses are tumor-destructive and immunostimulatory tools for therapy of solid tumors. They induce severe inflammations in tumor tissue[20–22] facilitating cross-presentation of tumor antigens and induction of antitumoral T-cells.[21,23,24] Therefore, oncolytic viruses are attractive means to support PD-1 immune checkpoint blockade.

In our study, we investigated whether localized tumor infection with an oncolytic adenovirus is capable of overcoming systemic tumor resistance to PD-1-immunotherapy. To investigate a broad spectrum of tumor-directed CD8 T-cell responses, we screened PD-1-resistant CMT64 cells for putative MHC class I neoepitopes. Using these neoepitope candidates, we showed that anti-PD-1 therapy alone was not able to elicit therapeutically relevant immune responses, whereas viral oncolysis induced significant CD8 T-cell cytotoxicity, directed against a conserved set of neoepitopes. Interestingly, PD-1-blockade during oncolytic virus infection led to significant spreading of the neoepitope-directed T-cell spectrum and facilitated successful tumor therapy. The synergy of localized virotherapy and systemic PD-1 blockade was confirmed in a transgenic model of cholangiocarcinoma. In this model, local oncolysis prevented tumor resistance to systemic anti-PD-1 treatment, leading to CD8-dependent eradication of lung metastases, which showed significant upregulation of PD-L1 in the primary tumor and metastases in response to viral tumor infection. Our results strongly suggest the clinical evaluation of virotherapy and PD-1 immunotherapy to improve therapeutic efficacy in tumors that are refractory to checkpoint blockade.

RESULTS

Virus-mediated tumor inflammation elicits CD8 T-cell responses directed against a set of neoepitopes derived from mutated genes

We aimed to investigate neoantigenome-wide antitumoral CD8 T-cell responses upon PD-1 checkpoint inhibition and/or virotherapy in an immunocompetent tumor model. For this purpose, we analyzed the mutanome of CMT64 lung adenocarcinoma cells. CMT64 tumors in syngeneic C57/BL6 mice do not respond to PD-1 immunotherapy by tumor-infiltration of immune cells opposed to therapy-sensitive Hepa1-6 cells as control (**Supplementary Figure S1**). CMT64 cells do not express PD-L1, which is consistent with the notion that PD-1 inhibition is known to work more effectively in tumors expressing PD-L1.[1]

As illustrated by the work-flow in **Figure 1a**, we analyzed the mutanome of CMT64 cells starting with transcriptomic sequencing. 274 nonsynonymous single-nucleotide variants (SNV) were detected, consistent with the frequency of mutations typically found in human lung tumors.[15] The complete list of all nonsynonymous SNVs, the corresponding mutated genes, and key features of derived neoepitopes are provided in **Supplementary Table S1**. We analyzed various peptide sequences harboring nonsynonymous SNVs for their capability to bind to H2-Kb and H2-Db using the SYFPEITHI-prediction algorithm.[25] We identified 44 putative neoepitopes in 35 genes with a binding score ≥20, which has been defined arbitrarily as a cutoff. All 44 predicted neoepitopes of CMT64 cells were synthesized as minimal binding-motif peptides (**Supplementary Table S2**) and neoepitope-specific CD8 T-cell responses were investigated by IFNγ-ELISpot analyses in CMT64-tumor bearing mice (**Figure 1b**). Consistent with the hypothesis that the neoepitope-spectrum of a mature tumor reflects the result of immunoediting processes, we did not detect spontaneous immune responses in tumor-bearing, but untreated mice. PD-1 inhibition elicited a weak but significant immune response specific for the neoepitope Ndufs1-V491A in all individuals (**Figure 1b**, marked by an asterisk). Since oncolytic viruses are known to provoke antitumoral immune responses, we investigated whether intratumoral injection of an oncolytic adenovirus (hTertAd) is capable of triggering neoepitope-specific CD8 T-cell responses. In our experiment, oncolytic virotherapy raised CD8 T-cell responses to at least 5 of 44 tested neoepitopes. Responses to H2-Q2-D244E, Ndufs1-V491A, Rab13-K196N, Ppat-I208M, and Gsta2-Y9H, were reliably elicited in all investigated individuals whereas responses to Chd2-T647A and Arhgef10-M207I were only detected in a subset of animals. Remarkably, the Ndufs1-V491A-specific response was triggered by PD-1 therapy and oncolysis. Neither tumor-free animals treated with PD-1 antibody nor untreated tumor-bearing mice showed a response to this epitope confirming the specific triggering of this tumor-directed response by the applied treatments (**Figure 1c**).

To exclude that detectable tumor-directed CD8 T-cell responses are due to cross-reactivity of antiviral immune responses, virotherapy was also administered by intraperitoneal injection. This route of application circumvents virus-mediated oncolysis and triggers robust viral T-cell immunity. In this setting, we observed no significant immune response to oncolysis-responsive neoepitopes (**Supplementary Figure S2a**). To investigate the potential of triggering autoimmune responses, cross-reactivity to corresponding wild-type peptides was evaluated in splenocytes from tumor-bearing mice following intratumoral oncolysis (**Figure 1d**). Although some of the calculated binding scores of mutated neoepitopes and their wild-type counterparts were almost similar (**Supplemetary Figure S2b**), the immune responses were significantly higher against neoepitopes confirming the specificity of tumor-directed immune responses for their mutated targets. We finally investigated the effect of PD-L1 expression on neoepitope-specific CD8 T-cell responses in isogenic experiments using stably transduced CMT64-PDL1 cells. These experiments demonstrated that the observed neoepitope-specific CD8 T-cell responses occurred independently of PD-L1 expression (**Supplementary Figure S2c,d**). A tabular overview containing a list of the detected virotherapy-responsive neoepitopes and essential information on the neoepitope and binding scores is provided in **Figure 1e**.

Neoepitope-specific CD8 T-cell responses raised by virus-mediated oncolysis have cytotoxic activity and exhibit improved therapeutic efficacy

First, we wanted to investigate whether neoepitope-specific CD8 T-cell responses can be triggered by alternative inflammatory agents. Therefore, we replaced oncolytic virus infection by the toll-like receptor (TLR)-ligands poly(I:C) and CpG that were injected i.t. into CMT64 tumors. In contrast to virotherapy, neither poly(I:C) nor CpG elicited a significant neoantigenome-directed immune response (**Figure 2**) suggesting that viral oncolysis plays an important role for triggering neoepitope-specific responses. A major functional parameter of tumor-directed CD8 T-cells is their ability to effectively kill their

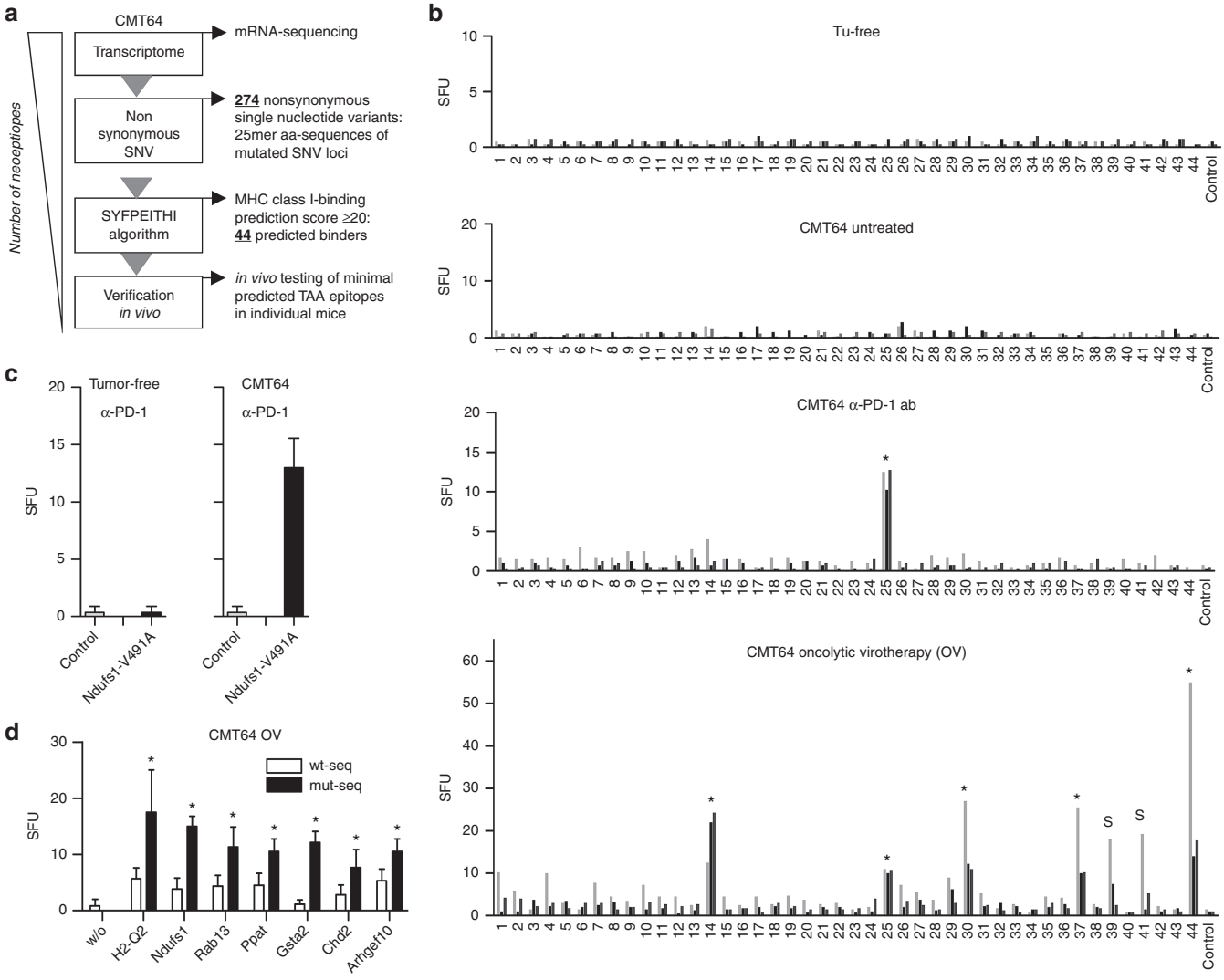

e

Immunodominant tumor-associated epitopes including a nonsynonymous single nucleotide variant of CMT64					
Gene i.d.	Gene name	Mutation	Min. sequence	Score	MHC-type
NM_010392	histocompatibility 2, Q region locus 2 (H2-Q2)	D244E	TWQLNGEEL	25	H2-Db
NM_145518	NADH dehydrogenase (ubiquinone) Fe-S protein 1 (Ndufs1)	V491A	AAVSNMVQKI	29	H2-Db
NM_026677	RAB13, member RAS oncogene family (Rab13)	K196N	SDKKNNKCL	22	H2-Db
NM_172146	phosphoribosyl pyrophosphate amido-transferase (Ppat)	I208M	DPYGNRPLCM	20	H2-Db
NM_008182	glutathione S-transferase, alpha 2 (Yc2) (Gsta2)	Y9H	LHHFNARGRM	22	H2-Db

Sporadically triggered tumor-associated epitopes including a nonsynonymous single nucleotide variant of CMT64					
Gene i.d.	Gene name	Mutation	Min. sequence	Score	MHC-type
NM_001081345	chromodomain helicase DNA binding protein 2 (Chd2)	T647A	APLQNSLKEL	27	H2-Db
NM_172751	Rho guanine nucleotide exchange factor (GEF) 10 (Arhgef10)	M207I	AWIENPEEAI	28	H2-Db

Figure 1 Oncolytic virotherapy elicits specific CD8 T-cell responses against a defined panel of neoepitopes in PD-1-resistant CMT64 tumors. (**a**) Work flow for prediction and identification of neoepitope-specific CD8 T-cell responses in CMT64 cells. (**b**) C57BL/6 mice with established s.c. CMT64-tumors were treated twice with αPD-1 antibody (days 0 and 3) or with intratumoral injection of hTertAd. Tumor-free and tumor-bearing mice without treatment served as controls. Splenocytes were harvested 1 week after the first treatment and used for analysis of neoepitope-specific CD8 T-cell responses. For this screen, 44 minimal epitopes from CMT64 sequencing were synthesized as minimal peptides to detect neoepitope-specific responses in IFNγ-ELISpot assays. CD8 T-cell responses observable in all investigated individuals are marked by an asterisk. Responses that were restricted to a subset of mice are marked with "s". The graph shows representative results from three mice of a total number of eight ($n = 8$ per group). (**c**) Ndufs1-V491A-specific CD8 T-cell responses were determined in tumor-free mice treated with a PD-1 blocking antibody and compared to responses in CMT64-tumor-bearing mice ($n = 5$ per group). Irrelevant peptides served as control. (**d**) To investigate the ability of neoepitope-specific CD8 T-cell responses to distinguish between tumor-associated neoepitopes and corresponding wild-type epitopes, splenocytes from mice after virotherapy treatment were stimulated with mutated epitope motifs or with corresponding wild-type peptides, respectively. Pooled splenocytes were used for analysis ($n = 5$ animals). (**e**) Tabular overview containing a list of detected virotherapy-responsive neoepitopes and additional key information.

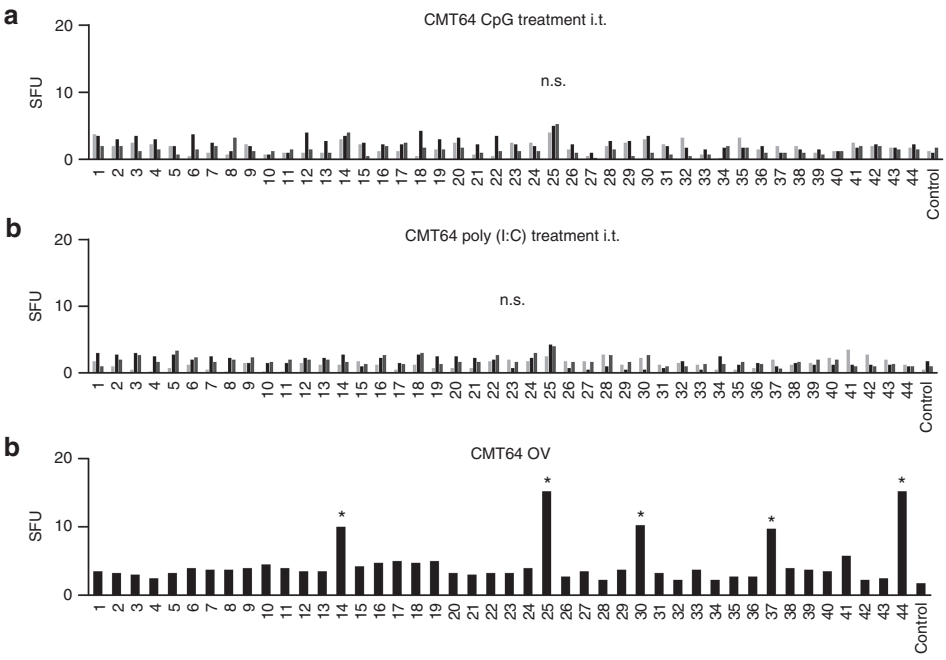

Figure 2 Intratumoral inflammation by toll-like receptor (TLR)-ligands is unable to trigger neoepitope-specific CD8 T-cell responses. (**a**) To investigate whether TLR-ligands can mimic the immunogenicity of viral oncolysis and are capable of triggering tumor-specific CD8 T-cell responses upon injection, mice received intratumoral treatment with the TLR-ligands CpG or poly(I:C), and oncolytic virus as positive control. The CMT64-derived peptide library was used to screen for putative tumor-responses by ELISpot analysis. Representative results of tumor-specific responses from three out of five mice treated with CpG-ODN are shown. (**b**) Likewise, the graph shows responses from three representative out of five animals treated with poly(I:C). (**c**) The figure shows ELISpot results from a mouse receiving intratumoral oncolytic virotherapy for the purpose of comparison.

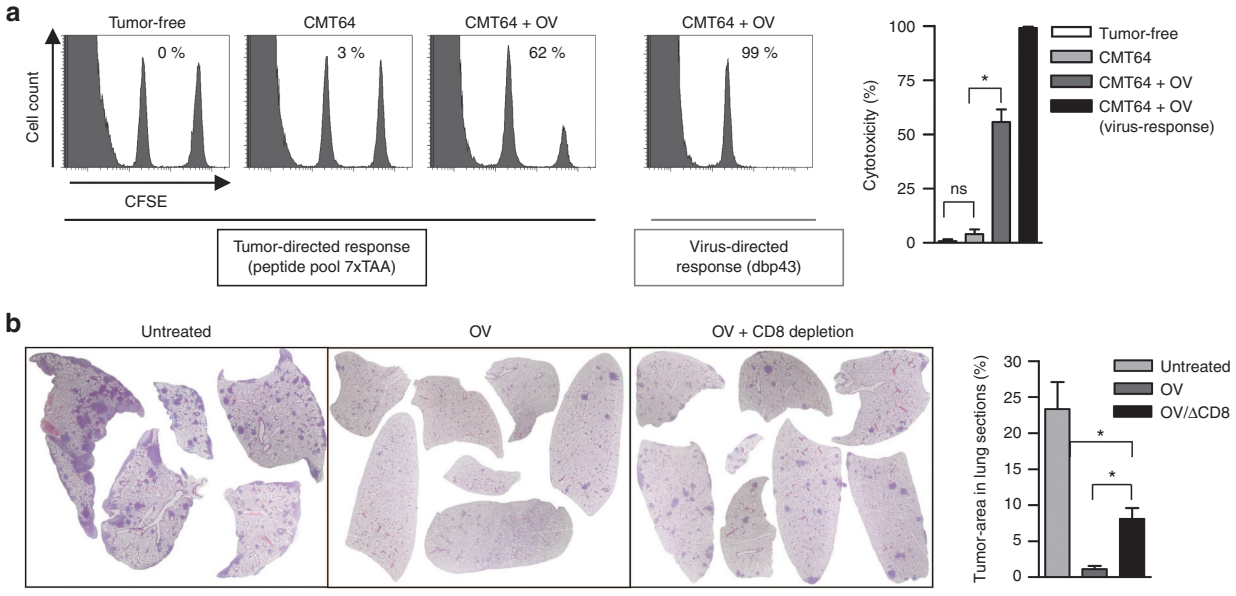

Figure 3 Virotherapy triggers cytotoxic neoepitope-specific CD8 T-cell responses and efficiently eradicates uninfected lung metastases. (**a**) C57BL/6 mice with subcutaneous CMT64 tumors were treated with or without oncolytic virotherapy. To determine cytotoxic activity of tumor-specific CD8 T-cells, an *in vivo* cytotoxic assay was performed by adoptive transfer of donor cells pulsed with a peptide pool consisting of all seven tumor-reactive epitopes triggered by oncolytic virotherapy. Cytotoxicity was calculated from ratios of the $CFSE^{hi}$-target peak pulsed with the tumor-specific peptide pool and the $CFSE^{lo}$-reference peak pulsed with irrelevant peptides. The virus-specific response to dbp served as positive control. Representative histograms are shown in the left panel. The right panel shows the calculated cytotoxicity of indicated groups. (**b**) Antitumoral efficacy of tumor-specific CD8 T-cells was investigated by clearance of pre-established CMT64 lung colonies. Mice received an i.v. injection of CMT64 cells to establish lung colonies and were treated with intratumoral injections of hTertAd. On day 18 after therapy, mice were sacrificed and lungs were prepared for histology. Untreated mice served as control. To assess the contribution of CD8 T-cells to the clearance of lung colonies, an additional group received virotherapy and CD8 depleting antibodies. The tumor-area of colonies was calculated by computer-based analysis from HE-stained lung sections. The ratio of tumor-area to total lung area is shown in the graph on the right side.

target cells. We investigated *in vivo* cytotoxicity by pulsing target cells with a peptide pool reflecting all seven oncolysis-responsive neoepitopes. Whereas untreated tumor-bearing mice did not display killing of neoepitope-labeled target cells, we observed significant cytotoxicity after virotherapy (**Figure 3a**). Finally, immune-mediated eradication of tumors was investigated in mice bearing a primary subcutaneous CMT64 tumor for intratumoral application of virotherapy and lung colonies to evaluate the immune-mediated antitumoral effects. These lung metastases remain uninfected when the virus is applied by intratumoral injection as shown previously.[21] Our results demonstrate that virus-mediated tumor infection strongly reduced the intrapulmonary tumor burden. CD8 T-cell depletion experiments confirmed that CD8 T-cell responses led to a significantly reduced tumor burden (**Figure 3b**). However, tumors in CD8-depleted mice did not reach the size that was observable in untreated mice, suggesting a role of further immune-mediated antitumoral mechanisms. Possibly, NK-cells can be stimulated by systemic cytokines upon viral infection to attack disseminated tumor cells since virotherapy-stimulated NK cells reduce metastasis after surgical tumor resection.[26] Furthermore, recent studies have shown that neoepitope-specific CD4 T cells can essentially contribute to antitumoral responses.[27,28]

Virus-mediated oncolysis during simultaneous anti-PD-1 immunotherapy broadens the spectrum of neoantigenome-specific T-cell responses and leads to increased PD-L1 expression by tumor-infiltrating antigen-presenting cells

PD-1 inhibition maintains the function of antigen-experienced peripheral T-cells suggesting that oncolysis-induced CD8 T-cell responses could be further enhanced by PD-1 immunotherapy. Since the specific T-cell response of Ndufs1-V491A was detectable after both single therapies, we selected this neoepitope for a quantitative investigation. Using a pentamer for specific T-cell receptor staining, we observed a comparable induction of Ndufs1-V491A-specific T-cell responses by anti-PD-1 treatment or virotherapy alone. Interestingly, combined treatment did not further elevate Ndufs1-V491A-specific responses (**Figure 4a**). Instead, we observed a strong spreading of immune responses to additional neoepitopes in more than half of all treated mice upon treatment combination (**Figure 4b**). When comparing individual animals, these additional neoepitope-specific responses had a rather randomized pattern in contrast to the regular patterns that we observed after single therapies. Additionally, the number of responsive neoepitopes varied between different individuals. However, at least three epitopes were additionally detectable in the majority of responding animals (**Supplementary Figure S3a**). Similar results were found in CMT64-PDL1 tumors confirming that PD-L1 expression by the tumor cells did not affect neoepitope-specific responses in this model (**Supplementary Figure S3b**). In total, 9 out of 16 animals responded with an extensive spreading of the immune response to 9–12 neoepitopes. Since these data showed that alterations in PD-L1 expression by the tumor cells were unlikely to play a role in broadening T-cell responses, we analyzed PD-L1 expression by antigen presenting cells (APC), defined by expression of $CD45c^+$ $CD11c^+$, in the lymphatic system (**Figure 4c**). When we investigated $CD45^+$ $CD11c^+$ cells in tumor-draining lymph nodes and nontumor-draining lymph nodes, we found high PD-L1 levels on APCs in tumor-draining lymph nodes but not in nontumor-draining lymph nodes. However, in all treatment groups including PD-1 blockade alone, PD-L1 was found to be highly expressed in both tumor-draining lymph nodes and nontumor-draining lymph nodes suggesting that all therapies were able to affect PD-L1 expression on APCs. Moreover, when we analyzed tumor resident APCs, we detected an increased expression of PD-L1 on antigen presenting cells after therapy that was statistically significant when virotherapy was involved and which was highest in the combined group. Since PD-L1 expression is an indicator of an immune-active microenvironment and also a surrogate marker for tumor response to PD-1 checkpoint inhibition[8] these findings show preferable immune activation when the tumor tissue is affected by viral oncolysis (**Figure 4d**). Consistent with this observation, we have previously shown in this tumor model that local tumor infection by an oncolytic virus induces effective cross presentation of tumor-specific antigens on tumor-infiltrating APCs.[21] In summary, these data indicate that local oncolysis plays an important role in shaping broad neoantigen-specific T-cell responses after virotherapy and PD-1 immunotherapy.

Localized virus-mediated tumor infection overcomes systemic resistance to PD-1 immunotherapy in syngeneic and transgenic mouse models

Next, we investigated whether localized oncolysis is capable of overcoming resistance to systemic PD-1 immunotherapy. To allow for detection of therapeutic synergy by PD-1 inhibition and intratumoral virotherapy we used a model of disseminated lung cancer with a higher initial tumor burden compared with the previous experiments. The therapeutic timeline, the setup of experimental groups, and time points for inspection of lung tumor burden are illustrated in **Figure 5a**. A growth curve of the treated primary CMT64 tumor revealed that PD-1 therapy or oncolytic virotherapy (OV) alone did not effectively inhibit tumor progression, whereas combined therapy was able to reduce the growth of this low immunogenic and aggressively growing tumor (**Supplementary Figure S4**). Inspection of the lung tumor burden showed that αPD-1-antibodies alone had no effect on metastases. Virus-mediated oncolysis alone was capable of reducing the tumor burden in the lung to a significant degree. Combined treatment led to significantly increased elimination of lung colonies, demonstrating the abrogation of systemic resistance of uninfected tumors to PD-1 immunotherapy by localized oncolysis (**Figure 5b**,**c**). Remarkably, half of the animals in the combination group showed an impressive tumor regression with almost complete elimination of lung colonies, whereas some animals with the same treatment did not eliminate lung tumors more efficiently than mice receiving virus alone. This finding correlates with the proportion of approximately 50% of animals that respond to combination therapy by spreading of CD8 T-cell neoepitopes as shown above. Survival monitoring displayed that combining virotherapy and PD-1 inhibition resulted in a significantly prolonged survival compared to the other treatment groups (**Figure 5d**). The improved survival of the combined treatment group also suggests that the therapeutic benefit was limited to half of the animals whereas other animals showed survival comparable to the virotherapy group consistent with the ratio of animals that respond by epitope-spreading. In CD8 knockout mice, we did not observe any difference between the treatment groups

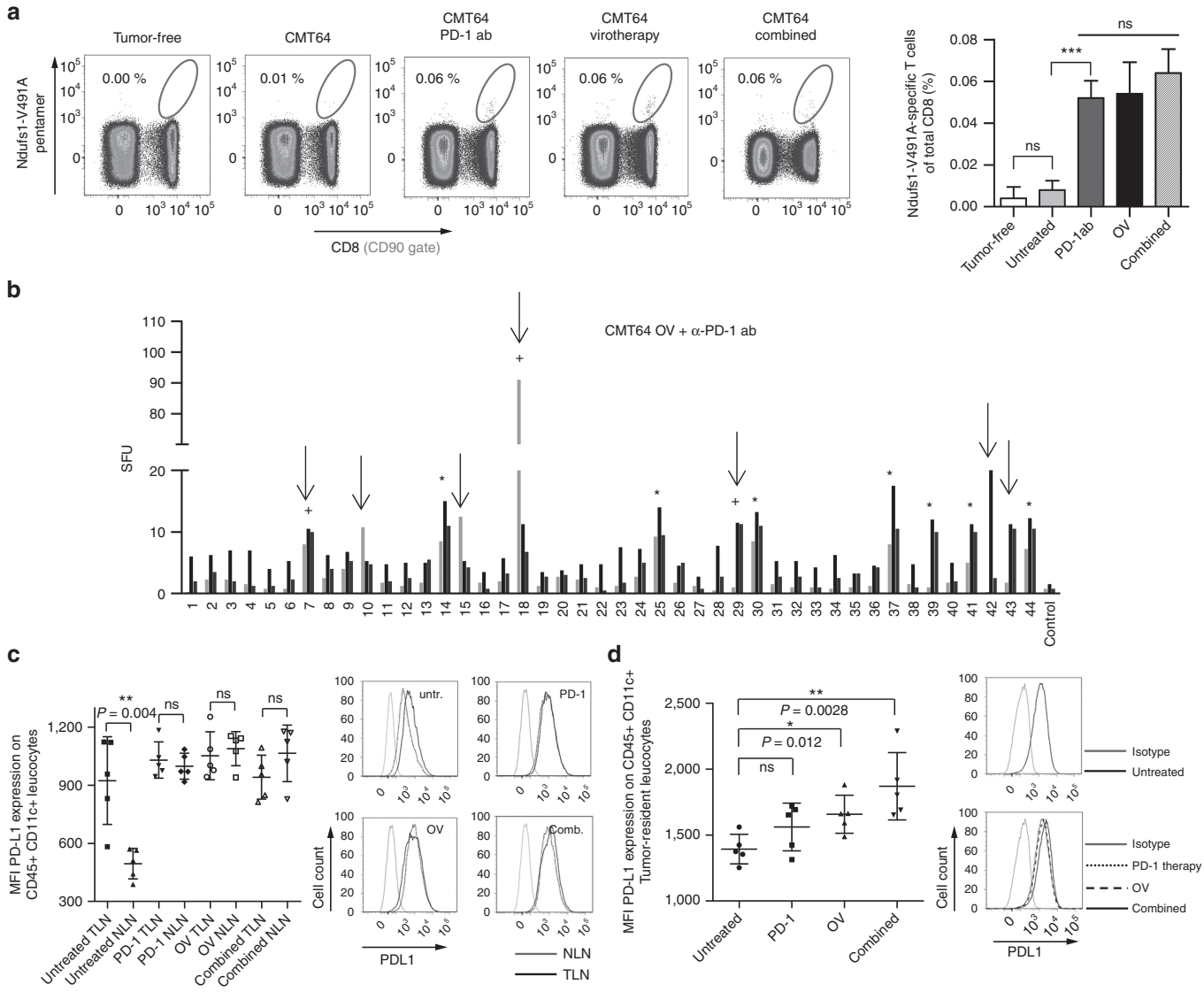

Figure 4 PD-1 inhibition during virus-mediated tumor inflammation broadens the epitope spectrum of neoantigenome-directed CD8 T-cell responses. (**a**) Using Ndufs1-V491A-specific pentamers for direct T-cell receptor staining, tumor-directed CD8 T-cell responses were monitored in mice after PD-1 checkpoint inhibition, oncolytic virotherapy, and a combination of both treatments. Tumor-free mice and untreated CMT64-tumor bearing mice served as controls. The gating in the representative dotplots (left panel) refers to Ndufs1-V491A-specific CD8 T-cells and the corresponding quantitative analysis is shown on the right panel. (**b**) Mice bearing s.c. CMT64-tumors received a combination of PD-1 checkpoint blockade (d0 and d3) and oncolytic virotherapy (n = 8). 7 days following virotherapy, mice were screened for neoantigenome-specific CD8 T-cell responses. Epitopes induced by virotherapy are marked by asterisks. Additionally detected T-cell responses, which were neither induced by PD-1 blockade nor by virotherapy alone, are indicated by arrows. Additional epitopes, which were observable in at least 50% of responding individuals are marked by a plus sign. (**c**) For each treatment group, CD45$^+$ CD11c$^+$ leukocytes were prepared from tumor-draining lymphnodes (TLN) and nontumor-draining lymphnodes (NLN) and PD-L1 expression was quantified by flow cytometry. For those cells derived from corresponding treatment groups, mean fluorescence intensity of PD-L1 is indicated in the graph on the left side. The right panel shows representative histograms. (**d**) Accordingly, tumor-resident CD45$^+$ CD11c$^+$ leukocytes were prepared from CMT64 tumor-tissue and PD-L1 expression was analyzed.

demonstrating that antitumoral effects mediated by viral oncolysis and combination with PD-1 inhibition were dependent on CD8 T cells (**Figure 5e**).

Since tumor transplant models do not fully reflect therapy resistance of autochthonous tumors, we investigated combined therapy in a low immunogenic mouse model of transgenic cholangiocarcinoma induced by local electroporation of oncogenic transposon plasmids.[29] Since it has been described that Akt2 supports metastasis,[30] we transferred a constitutively active form of Akt2 together with KRasG12V in p53fl/fl mice. Intrahepatic electroporation of plasmids as shown in **Figure 6a** reliably induced primary intrahepatic tumor-formation within 3 weeks. At day 42, lung metastases were detectable in 75% of mice (total n = 12) and could be visualized by immunohistochemical detection of phosphorylated ERK (**Supplementary Figure S5**). **Figure 6b** illustrates the procedure of local virus injection into the single tumor nodule 21 days after electroporation. HE-stained sections of the tumor show large oncolytic areas 3 days after virotherapy. This effect was durable since 3 weeks after virotherapy tumor-tissue integrity was not fully restored (**Figure 6c**). On the other hand, primary tumors were not well suited

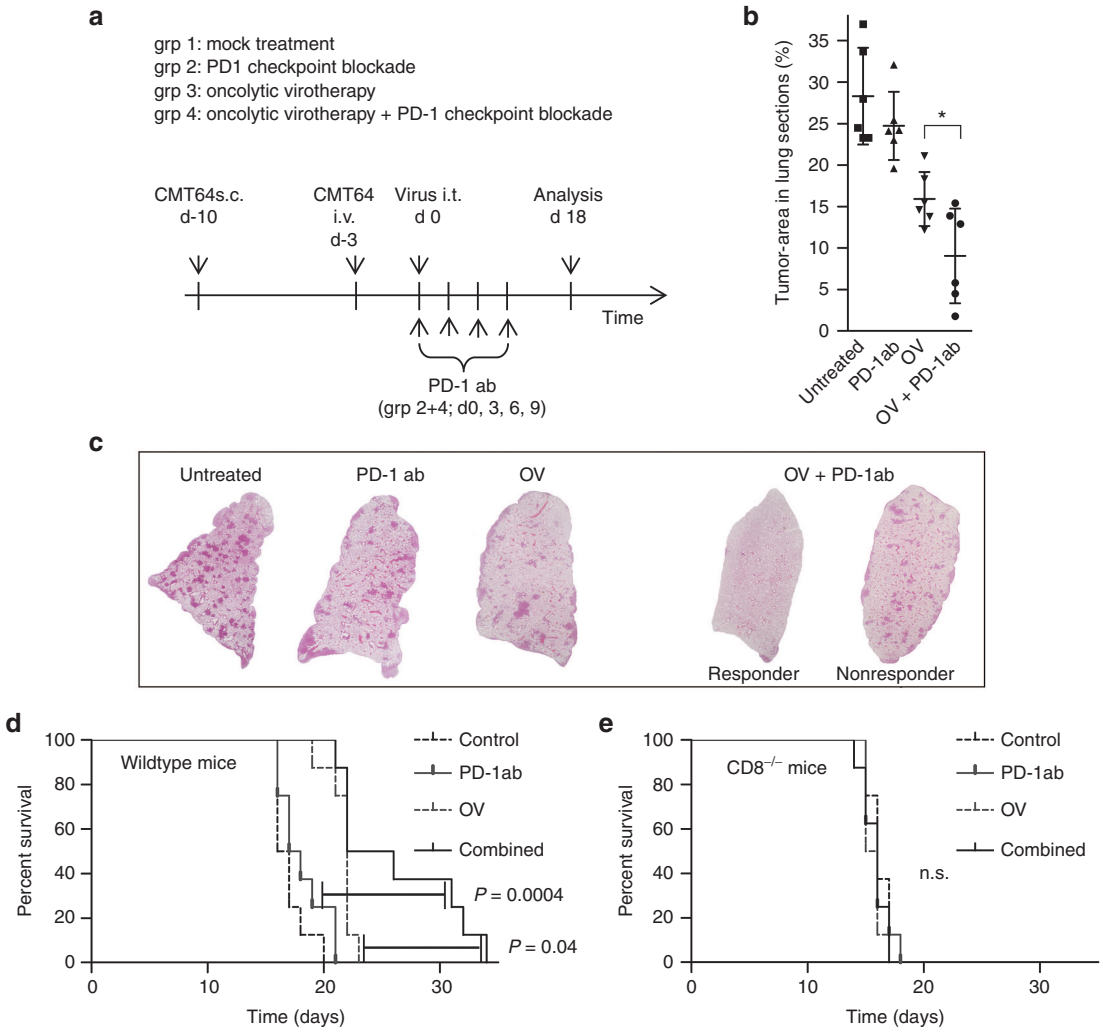

Figure 5 PD-1 checkpoint inhibition during virus-mediated tumor inflammation results in improved eradication of lung colonies. (**a**) Therapeutic efficacy of combined treatment with α-PD-1 ab and oncolytic virotherapy was assessed in a subcutaneous model of CMT64 including an increased intrapulmonary burden of metastasis (mice received an intravenous injection of 8×10^5 cells). The experimental timeline and the therapeutic groups are shown. Mice were treated by intratumoral virotherapy and/or α-PD-1 ab as described in the method section. (**b**) Mice were sacrificed on day 18 after development of lung colonies. Therapeutic efficacy was investigated histologically by measurement of the tumor area as described above. Combination therapy was significantly more efficient than the most effective monotherapy (virotherapy $P < 0.0188$). (**c**) Representative lung histologies are shown. (**d**) Therapeutic efficacy of combined treatment with αPD-1 antibody and oncolytic virotherapy was assessed by survival monitoring. Wild-type mice treated with both therapies demonstrate significantly prolonged survival compared to monotherapies. (**e**) The graph shows application of the same therapeutic scheme in CD8 knockout mice.

for size measurements due to the strong fibrotic tissue reaction upon viral lysis. To allow for an unbiased readout of immune-mediated antitumoral effects upon virotherapy and PD-1 checkpoint blockade, we monitored the noninfected lung metastases. The treatment regimen of the tumor-bearing animals is shown in **Figure 6d**. As shown in **Figure 6e,f**, application of PD-1 antibody alone was not sufficient to reduce the number of animals bearing lung metastases. Whereas oncolytic virotherapy alone showed antimetastatic activity to some degree, combined virotherapy and PD-1 inhibition led to the elimination of lung metastases in all investigated animals, demonstrating that localized oncolytic infection overcame resistance to systemic PD-1 immunotherapy in this murine model of cholangiocarcinoma. In agreement with the hypothesis that antitumoral activity was mediated by tumor-specific cytotoxic T-cells, CD8 depletion completely abrogated the elimination of metastases (**Figure 6f**). In this model, we investigated primary tumor and metastases for expression of PD-L1 (**Figure 6g,h**) as indicator of immune activation in response to treatment. Primary tumors in untreated and PD-1-treated mice only showed PD-L1 expression on infiltrating immune cells, but not on tumor cells. Interestingly, virotherapy resulted in upregulation of PD-L1 in the tumor tissue. Consistently, tumor cells of pulmonary metastases in untreated and PD-1-treated animals were PD-L1 negative, whereas tumor-resident immune cells, preferably located in the peripheral tumor zone, stained positive for PD-L1. In metastases as well, virotherapy resulted in a strong induction of PD-L1 on tumor cells that was still expressed three weeks after therapy.

In summary, our results demonstrate that intratumoral virotherapy provides excellent preconditions for concomitant PD-1 checkpoint blockade in PD-1 refractory tumors. Our data confirm the promising therapeutic efficacy of antitumoral T-cell

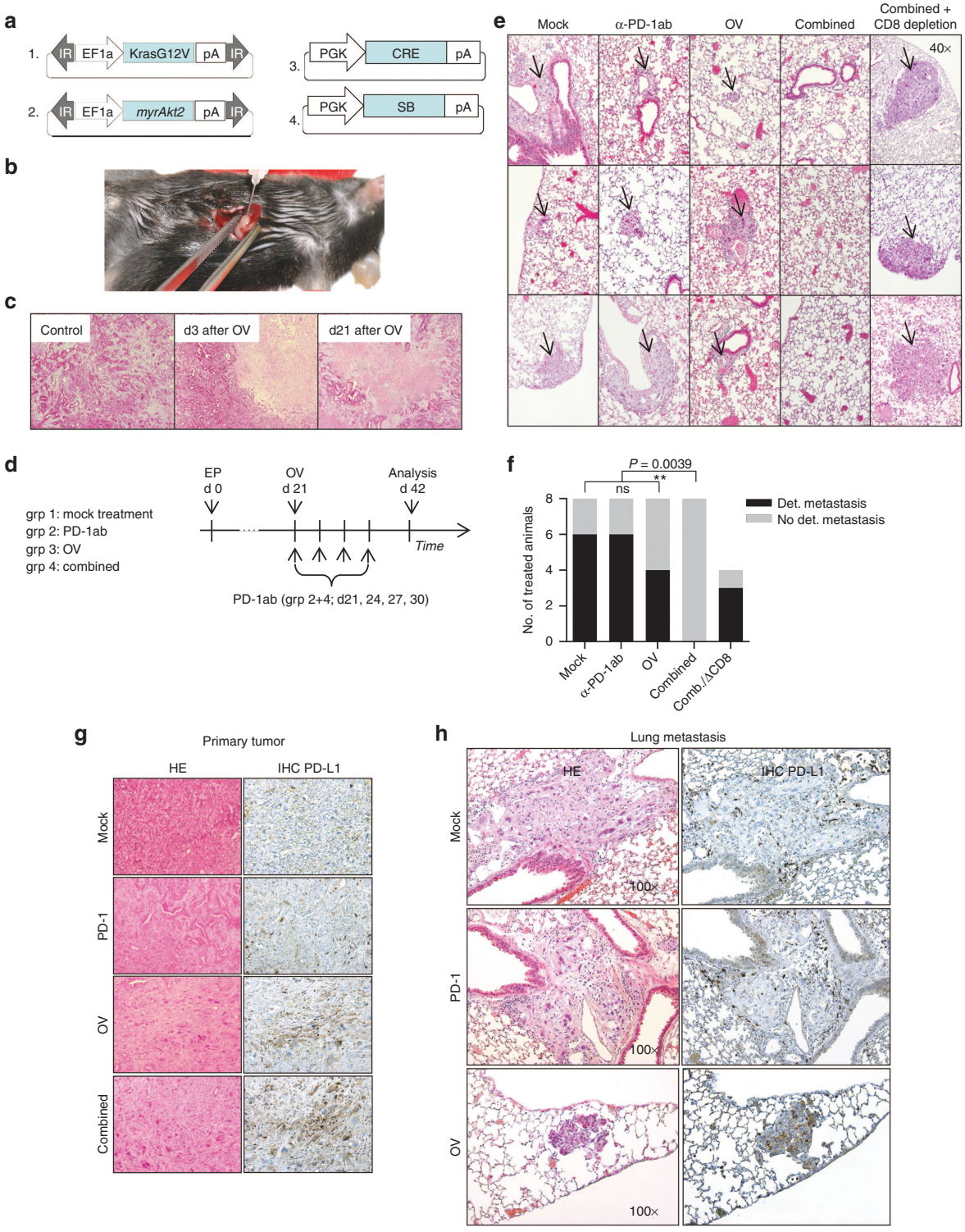

Figure 6 Viral oncolysis and concomitant PD-1 immunotherapy leads to complete elimination of spontaneous lung metastasis in a transgenic model of cholangiocarcinoma. (**a**) Transposon-based plasmids coding for KrasG12V and myrAkt2 and plasmids expressing SB13-transposase and Cre recombinase were used to establish locally restricted liver tumors by *in-situ* electroporation. On day 21 after tumor induction, mice developed a single nodule of cholangiocarcinoma suitable for intratumoral injections. (**b**) The photo illustrates the intratumoral application of virotherapy to the electroporation-induced liver tumor *in situ*. (**c**) Tumors were treated with intratumoral injection of hTertAd. On day 3 and day 21 after virotherapy, intratumoral lysis was investigated on HE-stained sections at 40-fold magnification. (**d**) Mice bearing intrahepatic tumors received a systemic administration of PD-1-blocking antibodies, intratumoral virotherapy, or a combination of both (n = 8 animals per group). For virotherapeutic application, mice were laparotomized and received intatumoral injections of virotherapy, or physiologic salt solution as control, respectively. Twenty-one days after treatment, lungs were screened for metastases. (**e**) Three representative lung histologies from each group are shown. (**f**) The graph displays the distribution of mice with detectable metastasis and metastasis-free mice for each treatment group according to the scheme shown in Figure 6d. An additional group treated with combined therapy received CD8-depleting antibodies (n = 4 animals). PD-L1 expression in primary tumors (**g**) and metastases (**h**) after different therapies as indicated was investigated by HE stainings and immunohistochemical staining (100-fold magnification).

responses in clinically relevant animal models of a transgenic and low-immunogenic tumor.

DISCUSSION

Increasing the tumor response rates to PD-1 checkpoint blockade remains an important clinical challenge and molecular factors that determine the therapeutic success of this promising therapy are incompletely understood. Since the success of checkpoint blockade has been associated with preexisting immune responses, strategies have been pursued to support antitumoral immune responses by additional vaccination against defined tumor antigens with rather disappointing results.[2,31]

The tumor mutanome has recently been suggested to be a suitable pool for the identification of targets for individualized vaccinations using tumor genome sequencing and bioinformatic prediction algorithms for immunogenic epitopes.[32] In our study, transcriptomic sequencing and neoepitope prediction in CMT64 lung cancer cells provided the basis for neoantigenome-wide analysis of CD8 T-cell responses upon virotherapy and/or PD-1 checkpoint blockade. Since oncolytic viruses are strong adjuvants per se they have already been successfully applied for expression of targeted antitumoral vaccines or cDNA libraries.[33–35] We further hypothesized that viral oncolysis could provide for induction of significant antitumoral immune responses to be further modulated by PD-1 checkpoint inhibition. Our results show that application of a PD-1 blocking antibody elicited an immune response against a single neoepitope (Ndufs1-V491A) that was not sufficient to inhibit tumor growth. In contrast, intratumoral application of an oncolytic virus was capable of inducing significant cytotoxic CD8 T-cell immune responses against a conserved set of neoepitopes. These belonged to protein families involved in highly conserved cellular processes such as antigen presentation (H2Q2), detoxification of xenobiotics (Gsta2), energy metabolism (Ndufs1), and membrane vesicle transport (Rab13) suggesting a possible contribution to malignant growth. In case of Ndufs1, it has recently been shown that molecular alterations in this metabolic pathway reflect tumor adaptation to low glucose levels.[36] The detected neoepitopes illustrate that immunogenic epitopes may correspond to genes with tumor-supporting functions which has implications for potential tumor immunoevasion upon epitope-targeted therapy. Instead of further enhancing the magnitude of single oncolysis-induced CD8 T-cell responses by PD-1 checkpoint blockade, we observed a significant spreading of T-cell responses to neoepitopes additional to those detectable after single therapies. Compared to the highly regular pattern after virotherapy, the extended pattern of T-cell responses after combined therapy varied significantly between different animals. Interestingly, broadened tumor-antigen directed CD8 T-cell responses have been recently observed in patients after treatment with the CTLA-4 inhibitor ipilimumab.[37]

PD-L1 is a strong indicator for ongoing immune-activation and a predictive marker for tumor response to PD-1/PD-L1 therapy.[8,9] We found an increase of PD-L1 levels on tumor-infiltrating APC that was significant in both groups receiving virotherapy and highest when virotherapy and PD-1 blockade were applied. These observations are consistent with our findings that localized oncolysis abrogated systemic resistance of uninfected tumors to PD-1 immunotherapy with a strong reduction of metastasis in the syngeneic CMT64 mouse model. Since we found that all therapies had equivalent effects on APCs in the nontumor-associated lymphatic system, local tumor inflammation and oncolysis appear to be crucial for immune activation and antimetastatic efficacy. Furthermore, we have previously shown that tumor virotherapy induces effective cross presentation of tumor-associated antigens by tumor-infiltrating APCs in the CMT64 model. Effective cross presentation of tumor antigens provides suitable preconditions for triggering broad neoantigen-directed T-cell responses. The important role of the local tumor inflammation and tumor cell lysis is consistent with a recent report demonstrating that localized infection of a subcutaneous tumor with oncolytic Newcastle disease virus converted a second contralateral tumor nodule into an inflammatory phenotype rendering the tumor sensitive to checkpoint immunotherapy.[38] Also, in a syngeneic mouse model of melanoma, a recent study showed an additional therapeutic benefit of CTLA-4 or PD-L1 inhibition, when antagonistic scFvs were expressed by an oncolytic measles virus.[39]

Tumors derived from cell lines with high mutational load are presumably much more immunogenic than transgenic cancers that are usually driven by a small number of dominant oncogenes. Therefore it is remarkable that the synergy of localized virotherapy and systemic PD-1 blockade was confirmed in a KRasG12V-transgenic mouse model of cholangiocarcinoma, which is a particularly low immunogenic tumor. Localized oncolysis overcame resistance of uninfected lung metastases to PD-1-immunotherapy in a CD8 T-cell-dependent manner. However, clinical response to checkpoint inhibition has not only been associated with the mutational load in tumors.[40] In the transgenic cholangiocarcinoma model used in this study, virotherapy and combined therapy strongly induced PD-L1 in tumor cells of primary tumors and metastases, indicating an immune-activated tumor microenvironment in these groups. The excellent antimetastatic activity observed in mice receiving virotherapy and PD-1 therapy is consistent with experience from clinical trials that PD-L1 expression in tumor cells represent a strong predictive factor for positive tumor response to therapies blocking the PD-1/PD-L1 pathway.[8,9]

Together these results further support the assumption that raising a multipronged immune attack is a promising approach to prevent tumor escape by epigenetic/genetic adaptation. The tumor neoantigenome harbors potential targets for personalized cancer vaccines and the identification of responsive neoepitopes will be a challenge for the design of tailored immunotherapies. Transcriptomic sequencing and epitope prediction can provide information about neoepitope candidates, but they still require validation *in vivo*. However, a critical spectrum of immunogenic neoepitopes for effective immunotherapies was neither detectable by PD-1 immunotherapy nor by TLR-ligands. Recently, Robbins *et al.*[41] used exomic sequencing and epitope prediction data for identification of immunogenic neoepitopes by adoptive transfer of tumor-infiltrating lymphocytes whereas others additionally employed mass spectrometry to verify MHC class I binding peptides.[42,43] Our findings demonstrate that intratumoral oncolysis is a suitable analytic tool to identify neoepitope-specific CD8 T-cell responses within a pool of predicted candidates thus combining both therapeutic and analytic functions.

In summary, our study shows that localized oncolytic infection abrogated resistance to systemic PD-1 immunotherapy by upregulating PD-L1 on tumor cells and by eliciting a broad-range

T-cell attack against the neoantigenome, which strongly supports further evaluation of this promising approach in clinical studies.

MATERIALS AND METHODS

Cells. Hepa1-6 and HEK293 cells were obtained from the American Type Culture Collection (ATCC, Manassas, VA). The lung adenocarcinoma cell line CMT64, originally established from a spontaneous papillary alveologenic tumor[44] was obtained from the European Collection of Cell Cultures (ECACC, Salisbury, UK). All cells were maintained in Dulbecco's Modified Eagle Medium (DMEM) + Glutamax, supplemented with 10% heat-inactivated fetal calf serum (all from Life Technologies, Carlsbad, CA), 100 units/ml penicillin, and 100 µg/ml Streptomycin (Seromed, Berlin, Germany) at 37 °C and 5% CO_2.

Mice. Six- to 8-week-old C57BL/6, p53fl/fl mice (Strain B6.129P2-Trp53^{tm1Brn}/J) and CD8 knockout mice (Strain B6.129S2-CD8a^{tm1Mak}/J) were used for experiments. All *in vivo* experiments were conducted according to the legal standards for animal care (TierSchG) with approval of the local authorities and the Hannover Medical School animal facility. We established s.c. CMT64 tumors by injecting 5×10^6 cells into the flanks of syngeneic C57BL/6 mice. Tumors were grown to a size of 100–150 µl prior to initial virus infection. PD-1 checkpoint inhibition was carried out by injection of 75 µg PD-1 blocking antibody per application. 100 µg CD8-specific antibody per injection was used to deplete CD8 T-cells. Lung colonies were induced by i.v. injection of 4×10^5 CMT64 cells 3 days prior to initial application of oncolytic virotherapy. I.v. injection of 8×10^5 cells was applied to establish a model with increased metastatic burden for experiments with combined oncolytic and PD-1 immunotherapy. Virotherapy was applied by a single intratumoral injection of 1×10^9 pfu hTertAd into CMT64- and transgenic tumors. Locally restricted transgenic tumors were established by *in vivo* electroporation of transposon-based plasmids as previously described.[29]

Transcriptome analysis combined with SNV calling. Total RNA was prepared from CMT64 and Hepa1-6 cells using RNeasy-Kit according to the manufacturer's protocol (Qiagen, Hilden, Germany). Quality and integrity of RNA was controlled on a 2100 Bioanalyzer (Agilent, Santa Clara, CA). The RNA sequencing library was generated from 1µg total RNA using TruSeq RNA Sample Prep Kits v2 (Illumina, San Diego, CA) according to the manufacturer's protocol. The libraries were sequenced on Illumina GA IIx using TruSeq SBS Kit v5-GA (110 cycles, paired ended run) with an average of 3×10^7 reads per RNA sample. Reads were aligned to the reference genome (C57BL/6) using open source aligner Tophat followed by Cufflinks[45] that assembles transcripts, estimates their abundances, and tests for differential expression and regulation. The GATK-Pipeline (GenomeAnalysisTK-1.5) was applied to alignment files for SNV calling.[46] SNV annotation was done using Annovar.[47]

Antibodies, peptides, TLR-ligands, and pentamers. The following mouse-specific antibodies were purchased from Biolegend (San Diego, CA): αIFN-γ clone AN-18, αIFN-γ biotin-conjugated clone R4-6A2, α-PD-1 clone RMP1-14 (LEAF format), CD8 FITC-conjugated and unlabeled (LEAF format) clone 53–6.7 and CD90.2 PerCP-conjugated clone 53-2.1. CD19-PE-Cy7 clone eBio1D3 and horse radish peroxidase-Avidin was purchased from eBioscience (San Diego, CA). All peptides were obtained from ProImmune (Oxford, UK) and are listed in the **Supplementary Material**. Virus-specific peptides are E1A (SGPSNTPPEI), E1B (VNIRNCCYI), and dbp43 (FALSNAEDL). Peptides were dissolved in DMSO to a concentration of 8 µg/µl.

For treatment with TLR-ligands, mice received i.t. 200 µg poly(I:C), or 50 µg CpG (ODN1826) in PBS as previously described.[21] To detect Ndufs1-V491A-specific T-cells, a custom-made H2-Db-restricted APC-labeled AAVSNMVQKI-specific pentamer was obtained from ProImmune.

Adenovirus preparation. The recombinant adenovirus hTertAd, used as standard oncolytic agent in this study, has been described before.[48] Adenoviral particles of hTertAd were prepared in HEK293 and purified by CsCl-banding according to standard methods. Infectious titers were determined using the Rapid Titer Kit (BD Biosciences, Franklin Lakes, NJ) following the manufacturer's recommendations. Endotoxin contaminations of viral preparations were controlled by LAL-Chromogenic Assay (Life Technologies). Virus stocks were stored at −20 °C in 25% glycerol, 10 mmol/l Tris-HCl (pH 7.4), and 1 mmol/l $MgCl_2$. Before use, viral preparations were dialyzed two times against physiologic buffer containing 10 mmol/l Tris (pH 8.0), 1 mmol/l $MgCl_2$, and 140 mmol/l NaCl at 4 °C.

Analysis of T-cell responses. To determine IFNγ-release from splenocytes activated by antigen-specific peptides, ELISpot-assays were performed as described before.[21] For measurement of tumor-specific responses, 2×10^5 splenocytes were used per well. Virus-specific responses for infection control were quantitated by use of 1×10^5 splenocytes per well. All graphs show absolute numbers of IFNγ-positive spot-numbers normalized to an input cell number of 2×10^5. To detect Ndufs1-V491A-specific CD8 T-cells, a customized H2-Db-restricted APC-labeled AAVSNMVQKI-specific pentamer was purchased from Proimmune and T-cell responses were investigated by flow cytometry using a FACS-Canto-II (BD Biosciences, Franklin Lakes, NJ). Analysis of flow cytometric data was performed using FlowJo7 software.

Antigen-specific cytotoxicity of T-cell responses was determined using carboxy-fluorescein-succinimidyl ester (CFSE)-labeled donor splenocytes in an *in vivo* cytotoxic T lymphocyte (CTL) assay as described.[49] Briefly, $CFSE^{hi}$ and $CFSE^{lo}$ cells were loaded with the antigenic peptides or an irrelevant peptide, respectively, prior to adoptive transfer in treated mice. After recovery of cells, the ratio between $CFSE^{hi}$ and $CFSE^{lo}$ cells was calculated to determine the antigen-specific cytotoxicity.

Histology and immunohistochemistry. Lung colonies, metastasis, and tumor-integrity were monitored by histology. For this purpose, mice were sacrificed and tissues (lung, liver, or tumor) were fixed with paraformaldehyde. Two-micrometer paraffin sections were stained with hematoxylin and eosin according to standard methods. PD-L1 stainings were performed by incubating sections with primary PD-L1 antibody (131073, polyclonal rabbit serum; Abcam, Cambridge, UK), secondary biotin conjugated goat antirabbit (7074; Cell Signaling Technology, Danvers, MA), streptavidin conjugated horse radish peroxidase (streptavidin-HRP), and 3,3'-Diaminobenzidine (DAB, both reagents from Life Technologies, Carlsbad, CA). For phospho-ERK1/2 stainings, sections were treated with 3% H_2O_2 and subsequently incubated with primary pERK1/2 (p44/42) antibody (4376, Cell Signaling), secondary biotin conjugated goat-anti-rabbit antibody, streptavidin-HRP, and DAB.

Plasmids. To establish a retrovirus coding for murine PD-L1, we generated a PD-L1 encoding DNA-fragment from cDNA of Hepa1-6 was amplified by a standard PCR using the Q5 polymerase (NEB, Ipswich, MA) and the primer pair 5′-AAGATATCATGGAGGATATTTGCTGGC-3′; 5′-AACTCGAGTTACGTCTCCTCGAATTG-3′. The resulting Fragment was then cloned into pQCXIX (BD Clontech). Likewise, the murine Akt2-gene was amplified from CMT64 cDNA by PCR using the primer pair 5′-CCTCTAGAATGAATGAGGTATCTGTCATCAAA-3′ and 5′-ttggatcctcactctcggatgctggctgagta-3′. The resulting fragment was subcloned in pBluescript and a myristylation sequence was added to obtain a constitutively active protein. myrAkt2 was inserted into the transposon plasmid pT3/EF1a plasmid (Xin Chen, UCSF, Addgene plasmid 31789). All sequences were validated by DNA-sequencing. All other constructs indicated in the figures have been described previously.[29]

Statistics. Data were analyzed by unpaired, two-tailed *t*-test when comparing two distinct experimental groups, and values are provided as mean ± SD, if not otherwise specified. Survival curves were analyzed by log-rank test. Statistical significance of metastasis-free mice in all groups was calculated by one-way ANOVA (analysis of variance) choosing Dunnett's post-test.

P values of 0.05 or less were considered statistically significant. GraphPad-Prism 5 (GraphPad Software, San Diego, CA) was used for analysis.

SUPPLEMENTARY MATERIAL

Figure S1. CMT64 cells are resistant to PD-1 immunotherapy and do not express PD-L1.

Figure S2. Characterization of neoepitope-specific CD8 T cell responses.

Figure S3. PD-L1-expression by CMT64 tumors does not affect epitope spreading after combined treatment.

Figure S4. Growth of the primary tumor following virotherapy and/or PD-1 inhibition.

Figure S5. Histologic visualization of lung metastasis in the transgenic model of cholangiocarcinoma.

Table S1. Complete list of single nucleotide variants identified in CMT64.

Table S2. List of peptides reflecting predicted neoepitopes in CMT64.

ACKNOWLEDGMENTS

This work was financially supported by the German Research Council (Deutsche Forschungsgemeinschaft/DFG: SFB-TRR77; WO 1933/1-1; GÜ 1508/1-1), German Cancer Aid (Deutsche Krebshilfe), and the Wilhelm-Sander-Foundation. N.W. designed and performed experiments, analyzed the data, prepared figures, and wrote the paper. N.W., E.G., B.F., A.S., S.K., and A.M.K. performed the experiments and collected data, R.G. performed sequencing and SNV determination, M.P.M. and T.C.W. provided material and reviewed the paper. S.K. and F.K. supervised research and wrote the paper.

REFERENCES

1. Topalian, SL, Hodi, FS, Brahmer, JR, Gettinger, SN, Smith, DC, McDermott, DF *et al.* (2012). Safety, activity, and immune correlates of anti-PD-1 antibody in cancer. *N Engl J Med* **366**: 2443–2454.
2. Hodi, FS, O'Day, SJ, McDermott, DF, Weber, RW, Sosman, JA, Haanen, JB *et al.* (2010). Improved survival with ipilimumab in patients with metastatic melanoma. *N Engl J Med* **363**: 711–723.
3. Brahmer, JR, Tykodi, SS, Chow, LQ, Hwu, WJ, Topalian, SL, Hwu, P *et al.* (2012). Safety and activity of anti-PD-L1 antibody in patients with advanced cancer. *N Engl J Med* **366**: 2455–2465.
4. Lynch, TJ, Bondarenko, I, Luft, A, Serwatowski, P, Barlesi, F, Chacko, R *et al.* (2012). Ipilimumab in combination with paclitaxel and carboplatin as first-line treatment in stage IIIB/IV non-small-cell lung cancer: results from a randomized, double-blind, multicenter phase II study. *J Clin Oncol* **30**: 2046–2054.
5. Powles, T, Eder, JP, Fine, GD, Braiteh, FS, Loriot, Y, Cruz, C *et al.* (2014). MPDL3280A (anti-PD-L1) treatment leads to clinical activity in metastatic bladder cancer. *Nature* **515**: 558–562.
6. Leach, DR, Krummel, MF and Allison, JP (1996). Enhancement of antitumor immunity by CTLA-4 blockade. *Science* **271**: 1734–1736.
7. Yuan, J, Adamow, M, Ginsberg, BA, Rasalan, TS, Ritter, E, Gallardo, HF *et al.* (2011). Integrated NY-ESO-1 antibody and CD8+ T-cell responses correlate with clinical benefit in advanced melanoma patients treated with ipilimumab. *Proc Natl Acad Sci USA* **108**: 16723–16728.
8. Taube, JM, Klein, A, Brahmer, JR, Xu, H, Pan, X, Kim, JH *et al.* (2014). Association of PD-1, PD-1 ligands, and other features of the tumor immune microenvironment with response to anti-PD-1 therapy. *Clin Cancer Res* **20**: 5064–5074.
9. Herbst, RS, Soria, JC, Kowanetz, M, Fine, GD, Hamid, O, Gordon, MS *et al.* (2014). Predictive correlates of response to the anti-PD-L1 antibody MPDL3280A in cancer patients. *Nature* **515**: 563–567.
10. Tumeh, PC, Harview, CL, Yearley, JH, Shintaku, IP, Taylor, EJ, Robert, L *et al.* (2014). PD-1 blockade induces responses by inhibiting adaptive immune resistance. *Nature* **515**: 568–571.
11. Lennerz, V, Fatho, M, Gentilini, C, Frye, RA, Lifke, A, Ferel, D *et al.* (2005). The response of autologous T cells to a human melanoma is dominated by mutated neoantigens. *Proc Natl Acad Sci USA* **102**: 16013–16018.
12. Matsushita, H, Vesely, MD, Koboldt, DC, Rickert, CG, Uppaluri, R, Magrini, VJ *et al.* (2012). Cancer exome analysis reveals a T-cell-dependent mechanism of cancer immunoediting. *Nature* **482**: 400–404.
13. Gubin, MM, Zhang, X, Schuster, H, Caron, E, Ward, JP, Noguchi, T *et al.* (2014). Checkpoint blockade cancer immunotherapy targets tumour-specific mutant antigens. *Nature* **515**: 577–581.
14. van Rooij, N, van Buuren, MM, Philips, D, Velds, A, Toebes, M, Heemskerk, B *et al.* (2013). Tumor exome analysis reveals neoantigen-specific T-cell reactivity in an ipilimumab-responsive melanoma. *J Clin Oncol* **31**: e439–e442.
15. Vogelstein, B, Papadopoulos, N, Velculescu, VE, Zhou, S, Diaz, LA Jr and Kinzler, KW (2013). Cancer genome landscapes. *Science* **339**: 1546–1558.
16. Sjöblom, T, Jones, S, Wood, LD, Parsons, DW, Lin, J, Barber, TD *et al.* (2006). The consensus coding sequences of human breast and colorectal cancers. *Science* **314**: 268–274.
17. Segal, NH, Parsons, DW, Peggs, KS, Velculescu, V, Kinzler, KW, Vogelstein, B *et al.* (2008). Epitope landscape in breast and colorectal cancer. *Cancer Res* **68**: 889–892.
18. Motz, GT and Coukos, G (2013). Deciphering and reversing tumor immune suppression. *Immunity* **39**: 61–73.
19. DuPage, M, Mazumdar, C, Schmidt, LM, Cheung, AF and Jacks, T (2012). Expression of tumour-specific antigens underlies cancer immunoediting. *Nature* **482**: 405–409.
20. Breitbach, CJ, Paterson, JM, Lemay, CG, Falls, TJ, McGuire, A, Parato, KA *et al.* (2007). Targeted inflammation during oncolytic virus therapy severely compromises tumor blood flow. *Mol Ther* **15**: 1686–1693.
21. Woller, N, Knocke, S, Mundt, B, Gürlevik, E, Strüver, N, Kloos, A *et al.* (2011). Virus-induced tumor inflammation facilitates effective DC cancer immunotherapy in a Treg-dependent manner in mice. *J Clin Invest* **121**: 2570–2582.
22. Grote, D, Cattaneo, R and Fielding, AK (2003). Neutrophils contribute to the measles virus-induced antitumor effect: enhancement by granulocyte macrophage colony-stimulating factor expression. *Cancer Res* **63**: 6463–6468.
23. Schulz, O, Diebold, SS, Chen, M, Näslund, TI, Nolte, MA, Alexopoulou, L *et al.* (2005). Toll-like receptor 3 promotes cross-priming to virus-infected cells. *Nature* **433**: 887–892.
24. Prestwich, RJ, Errington, F, Ilett, EJ, Morgan, RS, Scott, KJ, Kottke, T *et al.* (2008). Tumor infection by oncolytic reovirus primes adaptive antitumor immunity. *Clin Cancer Res* **14**: 7358–7366.
25. Rammensee, H, Bachmann, J, Emmerich, NP, Bachor, OA and Stevanović, S (1999). SYFPEITHI: database for MHC ligands and peptide motifs. *Immunogenetics* **50**: 213–219.
26. Zhang, J, Tai, LH, Ilkow, CS, Alkayyal, AA, Ananth, AA, de Souza, CT *et al.* (2014). Maraba MG1 virus enhances natural killer cell function via conventional dendritic cells to reduce postoperative metastatic disease. *Mol Ther* **22**: 1320–1332.
27. Kreiter, S, Vormehr, M, van de Roemer, N, Diken, M, Löwer, M, Diekmann, J *et al.* (2015). Mutant MHC class II epitopes drive therapeutic immune responses to cancer. *Nature* **520**: 692–696.
28. Tran, E, Turcotte, S, Gros, A, Robbins, PF, Lu, YC, Dudley, ME *et al.* (2014). Cancer immunotherapy based on mutation-specific CD4+ T cells in a patient with epithelial cancer. *Science* **344**: 641–645.
29. Gürlevik, E, Fleischmann-Mundt, B, Armbrecht, N, Longerich, T, Woller, N, Kloos, A *et al.* (2013). Adjuvant gemcitabine therapy improves survival in a locally induced, R0-resectable model of metastatic intrahepatic cholangiocarcinoma. *Hepatology* **58**: 1031–1041.
30. Rychahou, PG, Kang, J, Gulhati, P, Doan, HQ, Chen, LA, Xiao, SY *et al.* (2008). Akt2 overexpression plays a critical role in the establishment of colorectal cancer metastasis. *Proc Natl Acad Sci USA* **105**: 20315–20320.
31. Weber, JS, Kudchadkar, RR, Yu, B, Gallenstein, D, Horak, CE, Inzunza, HD *et al.* (2013). Safety, efficacy, and biomarkers of nivolumab with vaccine in ipilimumab-refractory or -naive melanoma. *J Clin Oncol* **31**: 4311–4318.
32. Castle, JC, Kreiter, S, Diekmann, J, Löwer, M, van de Roemer, N, de Graaf, J *et al.* (2012). Exploiting the mutanome for tumor vaccination. *Cancer Res* **72**: 1081–1091.
33. Bridle, BW, Stephenson, KB, Boudreau, JE, Koshy, S, Kazdhan, N, Pullenayegum, E *et al.* (2010). Potentiating cancer immunotherapy using an oncolytic virus. *Mol Ther* **18**: 1430–1439.
34. Kottke, T, Errington, F, Pulido, J, Galivo, F, Thompson, J, Wongthida, P *et al.* (2011). Broad antigenic coverage induced by vaccination with virus-based cDNA libraries cures established tumors. *Nat Med* **17**: 854–859.
35. Pulido, J, Kottke, T, Thompson, J, Galivo, F, Wongthida, P, Diaz, RM *et al.* (2012). Using virally expressed melanoma cDNA libraries to identify tumor-associated antigens that cure melanoma. *Nat Biotechnol* **30**: 337–343.
36. Birsoy, K, Possemato, R, Lorbeer, FK, Bayraktar, EC, Thiru, P, Yucel, B *et al.* (2014). Metabolic determinants of cancer cell sensitivity to glucose limitation and biguanides. *Nature* **508**: 108–112.
37. Kvistborg, P, Philips, D, Kelderman, S, Hageman, L, Ottensmeier, C, Joseph-Pietras, D *et al.* (2014). Anti-CTLA-4 therapy broadens the melanoma-reactive CD8+ T cell response. *Sci Transl Med* **6**: 254ra128.
38. Zamarin, D, Holmgaard, RB, Subudhi, SK, Park, JS, Mansour, M, Palese, P *et al.* (2014). Localized oncolytic virotherapy overcomes systemic tumor resistance to immune checkpoint blockade immunotherapy. *Sci Transl Med* **6**: 226ra32.
39. Engeland, CE, Grossardt, C, Veinalde, R, Bossow, S, Lutz, D, Kaufmann, JK *et al.* (2014). CTLA-4 and PD-L1 checkpoint blockade enhances oncolytic measles virus therapy. *Mol Ther* **22**: 1949–1959.
40. Snyder, A, Makarov, V, Merghoub, T, Yuan, J, Zaretsky, JM, Desrichard, A *et al.* (2014). Genetic basis for clinical response to CTLA-4 blockade in melanoma. *N Engl J Med* **371**: 2189–2199.
41. Robbins, PF, Lu, YC, El-Gamil, M, Li, YF, Gross, C, Gartner, J *et al.* (2013). Mining exomic sequencing data to identify mutated antigens recognized by adoptively transferred tumor-reactive T cells. *Nat Med* **19**: 747–752.
42. Yadav, M, Jhunjhunwala, S, Phung, QT, Lupardus, P, Tanguay, J, Bumbaca, S *et al.* (2014). Predicting immunogenic tumour mutations by combining mass spectrometry and exome sequencing. *Nature* **515**: 572–576.
43. Weinschenk, T, Gouttefangeas, C, Schirle, M, Obermayr, F, Walter, S, Schoor, O *et al.* (2002). Integrated functional genomics approach for the design of patient-individual antitumor vaccines. *Cancer Res* **62**: 5818–5827.
44. Franks, LM, Carbonell, AW, Hemmings, VJ and Riddle, PN (1976). Metastasizing tumors from serum-supplemented and serum-free cell lines from a C57BL mouse lung tumor. *Cancer Res* **36**: 1049–1055.
45. Trapnell, C, Roberts, A, Goff, L, Pertea, G, Kim, D, Kelley, DR *et al.* (2012). Differential gene and transcript expression analysis of RNA-seq experiments with TopHat and Cufflinks. *Nat Protoc* **7**: 562–578.
46. McKenna, A, Hanna, M, Banks, E, Sivachenko, A, Cibulskis, K, Kernytsky, A *et al.* (2010). The Genome Analysis Toolkit: a MapReduce framework for analyzing next-generation DNA sequencing data. *Genome Res* **20**: 1297–1303.
47. Wang, K, Li, M and Hakonarson, H (2010). ANNOVAR: functional annotation of genetic variants from high-throughput sequencing data. *Nucleic Acids Res* **38**: e164.
48. Wirth, T, Zender, L, Schulte, B, Mundt, B, Plentz, R, Rudolph, KL *et al.* (2003). A telomerase-dependent conditionally replicating adenovirus for selective treatment of cancer. *Cancer Res* **63**: 3181–3188.
49. Mueller, SN, Jones, CM, Smith, CM, Heath, WR and Carbone, FR (2002). Rapid cytotoxic T lymphocyte activation occurs in the draining lymph nodes after cutaneous herpes simplex virus infection as a result of early antigen presentation and not the presence of virus. *J Exp Med* **195**: 651–656.